

Memorandum on Hourly Sea Level Projections

Interim Deliverable for EPC-20-006, Prepared by:

Sam Iacobellis, Daniel Cayan²

November 2024

- This research is funded by the California Energy Commission (CEC) through its Electric Program Investment Charge (EPIC) Program, which invests in scientific and technological research to accelerate the transformation of the electricity sector to meet the state's energy and climate goals.
- The applied research grant, EPC-20-006, will integrate the latest downscaling approaches applied to the recently produced global climate models (GCMs) with an engagement process to develop a robust, usable, set of climate projections applicable for California.
- This memo is being shared to support transparent and timely consideration of interim deliverables that are relevant for energy stakeholders and all those interested in California's next generation of climate projections.

This memorandum is submitted to the CEC by UC San Diego's Scripps Institution of Oceanography. The memo meets deliverable requirements under Task 7 of the California Energy Commission's applied research grant EPC-20-006: Hourly Sea Level Rise Projections.

1. Introduction

Hourly projections of total resting sea level (still water; below represented as H_{SUM}), were produced at 13 sites in California, including four within San Francisco Bay (see Figure 1). The approach (section 2) relies on robust historical data (Table 1) from tide gauges that measure the height of the water at that location and uses these historical relationships to develop future still water levels based on tides, long-term sea level rise and meteorological/climate contributors. These data do not include the impact of waves. Still water level projections were produced for sites having long-term (~20 years or more) historical hourly water level observations from National Oceanographic and Atmospheric Administration (NOAA) water gauge instrumentation. Additional tide gauge locations further inland in the Sacramento/San Joaquin Delta were not included in the set of projections because they are so heavily influenced by freshwater inputs, especially during flood events (Bromirski and Flick 2008).



Figure 1. Sites of the 13 California tide gauge stations used in this study (note that Port Chicago is in the Sacramento-San Joaquin Delta, despite looking “land based” on the map)

2. Methods and Data

The water level at any given time is a superposition of several independent components each with its own variability and temporal signature (**Table 1**). The most predictable of these components is the astronomical tide produced primarily through the gravitational interactions of the Earth, Moon and Sun. Other components less predictable include changes in water level due

to meteorological forcing (winds, pressure, temperature near the ocean surface) along with large-scale secular trends in global sea level due to climate change. Thus, the still water level (H_{SUM}) at a selected location at any given time can be written as:

$$H_{SUM}(t) = H_{AST}(t) + H_{SLR}(t) + H_{MET}(t)$$

where, H_{AST} is the astronomical tide, H_{SLR} is the contribution from long-term sea level rise, and H_{MET} is the component due to meteorological forcing. Tide predictions are developed from tidal harmonic predictions (tidesandcurrents.noaa.gov), and the long-term rise scenarios are prescribed from recent external sea level rise assessments (California Ocean Protection Council, California Ocean Science Trust 2024).

H_{MET} includes meteorological and short period climate driven components, whose strongest amplitudes occur during large storms and often during El Nino/Southern Oscillation episodes (Flick, 1986; Flick 1988; Bromirski et al. 2003). H_{MET} is derived using a regression model approach employing weather and short period input from the sequence of weather and climate patterns from global climate model projections (Cayan et al., 2008). Being that the same climate model weather sequence is employed to develop downscaled weather and modeled surface hydrologic variability over California, the sequences of sea level fluctuations and coastal and terrestrial weather and hydrology are self-consistent—this distinguishes the present temporally explicit methodology from alternative statistical approaches (e.g. Thompson et al. 2021), that have been employed to model measures of sea level height along the California coast as well as a much broader set of tide gauges throughout the U.S.

The regression model workflow does not include the vertical motions from tectonics or other forms of land uplift or subsidence, but an allowance for these vertical processes is included in the tide gauge station-based projections of H_{SLR} (see section 2.2 below). And furthermore, the above equation for water level height does not include any effects due to wave run-up.

2.1 Astronomical Tide (H_{AST})

Coastal and San Francisco Bay locations in California generally have a mixed semi-diurnal tide regime (Flick, 2000), experiencing two high and two low tides of different amplitude every lunar day. The astronomical tides are predicted with good precision based on known tidal constituents (Zetler and Flick, 1985). In this study, hourly values of historical and future astronomical tides at each water gage location were obtained from the National Oceanographic and Atmospheric Administration (NOAA) website (tidesandcurrents.noaa.gov) which employs a tidal prediction program that actually solves for a set (between 20-30) of tidal constituents, covering a range of frequencies from sub-daily to multi decadal, with amplitude and phase derived from past observations. These tidal predictions are referenced to mean sea level values observed during the current National Tidal Datum Epoch (NTDE) of 1983-2001. Corrections for apparent secular increases in the amplitude of the tide (Flick et al., 2003) were not included because these increases are non-uniform along the Pacific coast, are relatively small, and may not be stable over the next several decades.

2.2 Long-term Sea Level Rise (H_{SLR})

Three contrasting projections of long-term sea level rise follow a selected set of low, intermediate, and high sea level rise scenarios as adopted by the California Sea Level Rise Guidance (2024). The sea level scenarios are derived from the sets of projections developed in the Intergovernmental Panel on Climate Change Sixth Assessment report (IPCC, 2021) and reflect an up-to-date scientific understanding of the physical drivers of sea level rise. The scenarios employed here are drawn from the same scenarios employed in the recent Federal multi-agency Sea Level Report (Sweet et al., 2022), and are also amongst those employed in California’s recent Sea Level Rise Guidance Update (California Ocean Protection Council, 2024).

As noted in the California Ocean Protection Council guidance “... Sea Level Scenarios are constructed and presented for California. Adopting the scientific framework and approach used in the 2022 Federal Sea Level Rise Technical Report and creating consistency between state and federal planning, each scenario is defined and labeled according to a target value of global mean sea level rise in 2100 (e.g., the Intermediate Scenario has a GMSL target of 1.0m (3.3ft)). The Sea Level Scenarios are derived from the sets of probabilistic projections developed in the Intergovernmental Panel on Climate Change Sixth Assessment report (IPCC AR6), and reflect the most up to date scientific understanding of the physical drivers of sea level rise. The Sea Level Scenarios for California span the plausible range of future sea level rise under all emissions and global development futures and enable users to consider sea level rise without first selecting a single emissions future on which to base planning and projects.”

Vertical land motion is incorporated into the sea level scenarios for each water level gauge location (California and is a primary driver of local variations in sea level rise across California (California Ocean Protection Council, 2024). Figure 2 shows the resulting low, intermediate, and high sea level scenarios as a function of time at the San Francisco site. Also included in Figure 2 is the observed historical annual mean still water level from 1950 through 2020.

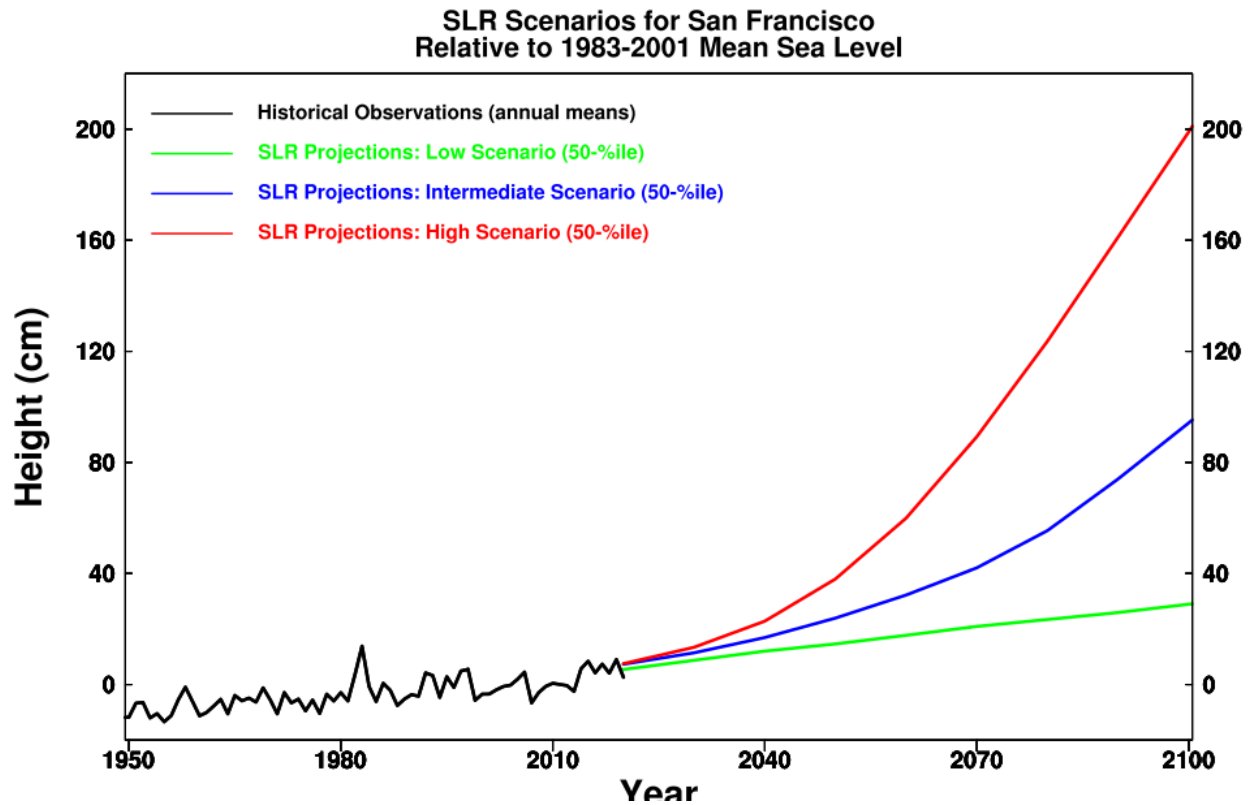


Figure 2. Sea level rise scenarios for the San Francisco tide gauge station site.

2.3.1 Meteorological Forcing (H_{MET}): Regression Model Development

At each tide gauge station site, the hourly residual water level is found by subtracting the predicted astronomical tide from the observed water level. A long-term trend is then computed using a linear best-fit through the residual water level values. These values, which are taken to represent the observed daily H_{MET} component, are computed by removing the long-term trend from the daily mean residual water level.

Note that when the regression model is applied to the climate model simulated data to calculate the weather component, the astronomical component and the low frequency sea level component is added in to yield the resultant still water level. Thus, the data can be decomposed into three different variables for further investigation if of interest.

For each of the 13 sites, a separate linear regression model was developed (**Table 2**) to relate historical non-tidal sea level residuals (Bromirski et al. 2003) to local sea level pressure (SLP), offshore wind stresses, local temperature near the sea surface (SST), and NINO 3.4 SSTs (SST averaged over 120°W-170°W, 5°S-5°N as a measure of the El Niño/Southern Oscillation (ENSO) component). A separate model was constructed for each individual tide gauge station.

The regression models were developed using historical water level observations from the individual NOAA tide gauge stations as the predictand, while the predictors were derived from downscaled ERA5 (Fifth Generation European Centre for Medium Range Weather Forecasts

(ECMWF) Reanalysis) products (Hersbach et al., 2023). The downscaling was applied using the LOCA framework developed by Pierce et al. (2018).

Individual climate models generally produce different climatological means for any particular region which could lead to significant discrepancies in the regressed estimates of H_{MET} . For example, the climatological wind speed at a certain location might differ between observations and reanalysis and/or the various climate models. To address this potential problem, the regression models were constructed to utilize anomalies of the various meteorological quantities, thus reducing biases that may develop due to different climatological means. Statistics of high (99.99 percentile) still water level, astronomical water levels, residual (from astronomical component) water level and trends are provided in Table 1 for each of the 13 station sites.

The time series of each variable was first detrended then anomalized by removing the annual cycle smoothed with a 31-day running mean filter. The annual cycle was removed since the astronomical tides include annual and semi-annual terms.

The regression models were constructed using the detrended and anomalized data extracted for the odd years of the tide data record (all available years between 1950-2020), and then evaluated using independent data from the even years of that record. Table 2 shows the squared correlation between observed and modeled daily mean residual water level during the evaluation period (even years) together with the standardized regression coefficients for each of the 13 sites.

Table 1. Observed still water level statistics during historical 1950-2020 period.

Site	Data Range	SL Trend (mm yr ⁻¹)	99.99%-ile still water level (meters)	99.99%-ile Astro Tide (meters)	99.99%-ile H_{MET} (meters)	Max still water level (meters)	Max H_{MET} (meters)
Crescent City	1950-2020	-0.89	1.74	1.51	0.97	2.15	1.42
Humboldt Bay	1993-2020	5.19	1.70	1.51	0.70	1.86	0.99
Point Arena	1996-2020	2.52	1.55	1.32	0.78	1.70	1.09
Port Chicago	1980-2020	1.55	1.41	1.06	0.92	1.66	1.12
Richmond	1996-2020	3.44	1.46	1.23	0.80	1.69	0.94
San Francisco	1950-2020	1.94	1.38	1.22	0.62	1.74	0.91
Alameda	1979-2020	0.70	1.56	1.34	0.69	1.84	0.85
Redwood City	1997-2020	2.90	1.75	1.57	0.72	1.99	1.21
Monterey	1974-2020	1.69	1.35	1.22	0.47	1.58	0.62
Port San Luis	1950-2020	0.98	1.34	1.26	0.69	1.60	1.26
Santa Barbara	1996-2020	2.54	1.36	1.28	0.49	1.44	0.58
Los Angeles	1950-2020	1.33	1.39	1.32	0.39	1.53	0.69
La Jolla	1950-2020	2.25	1.36	1.31	0.36	1.47	0.70

Notes:

- Water level (WL) values are still water levels relative to mean sea level (MSL)
- Extreme still water level values calculated after observed tide gauge water level was detrended
- Astronomical tides from 1983-2001 epoch used
- Known tsunami events removed from observed record (1964, 2010, 2011)

Table 2. Regression model statistics and regression model standardized coefficients, from model developmental (historical) 1950-2020 period. The 99.99%-ile water level and the range of maximum still water level were calculated by applying the regression model with data from the 38 SSP370 CMIP6 ensemble members during the historical period.

Site	Latitude	R ²	99.99%-ile still WL (meters)	Max still WL (meters)	Standardized Regression Coefficient				
					SLP	SST	U-wind	V-wind	Nino3.4
Crescent City	41.7°N	0.73	1.79	1.97 - 2.28	-0.62	0.15	0.12	0.30	0.14
Humboldt Bay	40.8°N	0.74	1.73	1.85 - 2.25	-0.65	0.14	0.09	0.23	0.26
Point Arena	38.9°N	0.64	1.54	1.72 - 2.05	-0.62	0.12	0.06	0.22	0.31
Port Chicago	38.1°N	0.49	1.39	1.59 - 2.02	-0.41	0.18	0.29	0.39	0.20
Richmond	37.9°N	0.66	1.38	1.56 - 1.89	-0.51	0.18	0.14	0.35	0.29
San Francisco	37.8°N	0.62	1.42	1.61 - 1.97	-0.57	0.17	0.10	0.30	0.25
Alameda	37.8°N	0.64	1.52	1.66 - 2.04	-0.54	0.21	0.11	0.28	0.27
Redwood City	37.5°N	0.62	1.68	1.85 - 2.19	-0.56	0.16	0.07	0.19	0.32
Monterey	36.6°N	0.68	1.34	1.47 - 1.76	-0.59	0.17	0.07	0.21	0.35
Port San Luis	35.2°N	0.54	1.38	1.50 - 1.84	-0.53	0.17	0.03	0.20	0.35
Santa Barbara	34.4°N	0.48	1.37	1.51 - 1.92	-0.44	0.17	0.04	0.13	0.53
Los Angeles	33.7°N	0.48	1.39	1.49 - 1.81	-0.50	0.14	-0.02	0.12	0.42
La Jolla	32.9°N	0.45	1.37	1.46 - 1.75	-0.45	0.13	-0.04	0.09	0.45

Notes:

- Still WL values are water levels relative to mean sea level (MSL)
- Extreme still water level values calculated after observed water level was detrended
- Astronomical tides from 1983-2001 epoch used
- Known tsunami events removed from observed record (1964, 2010, 2011)

During the development phase of the regression model several additional quantities were considered (e.g., Pacific Decadal Oscillation index, atmospheric geopotential height) as potential explanatory variables, but were not included in the final model due to relatively low significance (magnitude of standardized regression coefficient <0.05) in predicting the meteorological component of residual water level.

2.3.2 Meteorological Forcing (H_{MET}): Projections using CMIP6 Model Output

Projections of the meteorological component (H_{MET}) were produced by applying the regression models developed above with forcing data derived from Climate Model Intercomparison Project version 6 (CMIP6) earth system model (ESM) data. Vector wind was a LOCA2 downscaled product (Pierce et al., 2023). The derivation of H_{MET} from the CMIP6 variables is a key attribute of the projections because it yields daily sea level anomalies that have temporal sequences that are aligned with the surface meteorological and hydrological variations that are generated by the same CMIP6 climate models via LOCA2 downscaling and the related hydrological modeling. Thus, the resulting sea level projections will support a set of important diagnostic investigations, including those involving compound coastal ocean and coastal atmosphere and land surface variations.

Eleven CMIP6 models were employed, each containing one or more ensembles over three emission trajectories (Table 3). These eleven models are the subset of the 15 GCMs employed in California downscaled projections, for which each of the required meteorological and climate variables were available (each of the models that were not included suffered from one or more

missing variables). The CMIP6 output extends from 1950-2100, with greenhouse gas concentrations specified from observational sources during 1950-2014 and by the emission trajectories for 2015-2100. In this study, the historical period is defined as 1950-2020 to conform with the onset of the long-term sea level rise (H_{SLR}) projections that start in 2020. Thus, the first six years of the CMIP6 projections (2015-2020) are considered as part of the historical period.

Table 3. CMIP6 Global climate model (GCM) / Earth system model (ESM) projections that were employed to produce the set of H_{MET} projections that enter into the sea level rise projections in this project.

Model Name	Institution Home	Number of Ensembles per SSP Trajectory		
		SSP 245	SSP 370	SSP 585
ACCESS-CM2	Australia	1	1	1
CNRM-ESM2-1	France	1	1	1
EC-Earth3-Veg	Europe	5	4	4
EC-Earth3	Europe	3	2	3
GFDL-ESM4	United States	1	1	1
HadGEM3-CG31-LL	United Kingdom	1	0	3
INM-CM5-0	Russia	1	5	1
IPSL-CM6A-LR	France	5	10	4
MIROC6	Japan	3	3	5
MPI-ESM1-2-HR	Germany	2	6	2
MRI-ESM2-0	Japan	1	5	1
	Total	24	38	26

Values of H_{MET} can vary significantly over the course of a day and extreme flooding events may occur if maximum values of H_{MET} co-occur with an astronomical high tide. To better capture these potential flooding events hourly regressed estimates of H_{MET} are produced by disaggregating the daily forcing data from the CMIP6 climate models to hourly values using the method described in Cayan et al. (2008). Hourly values of the wind stress and temperature terms are determined using linear interpolation between daily values, while nearby historical coastal airport observations were employed to develop a statistical database used to specify hourly variation of SLP.

Finally, the regressed values of H_{MET} from each climate model and at each site are multiplied by a constant value to ensure that the modeled variability (as measured by the standard deviation of H_{MET}) during the historical period is the same as observed.

3. Extreme Sea Level Events

H_{SUM} , total still water level, is the sum of H_{MET} , H_{AST} and H_{SLR} . Importantly, many of the largest meteorological events affecting the West Coast have durations greater than 12 hours, so they are bound to produce effects that occur together with a daily high tide (Bromirski et al., 2017). To understand the makeup of projected high total water events, extreme sea level occurrences for La Jolla and San Francisco are illustrated as representative examples.

The frames in **Figures 3 and 4** illustrate contributions of H_{AST} and H_{MET} to all 99.99 percentile H_{SUM} events in each year from each of the SSP370 models that occurred under the intermediate sea level rise scenario.

In the current period, for the 99.99 percentile H_{SUM} events at La Jolla the mean H_{AST} contributions for these extremes is about 90% of the H_{SUM} , which amounts to events at or above 1.37m above historical mean sea level (**Table 1**), but decline to approximately 67% of H_{SUM} by 2080. In the current period, La Jolla mean H_{MET} contributions average about 15% and decline to an average of about 2% by 2080, but ranges greatly between/across 99.99 percentile H_{SUM} events. In the future, some events still feature high fraction H_{MET} contributions but as SL rises by 2040. And, as time progresses, there is an increasing occurrence of some events for which H_{MET} contributes negatively to H_{SUM} , owing to extreme H_{AST} occurrence and the growing contribution of H_{SLR} .

In the current period, San Francisco mean H_{AST} contributions to 99.99 percentile events (at or above 1.42 m above mean sea level; **Table 1**) average about 75%, but decline to approx 65% by 2080. In the current period, San Francisco mean H_{MET} contributions to 99.99 percentile H_{SUM} events average about 25%, but decline to about 5% by 2080.

In any particular year, the projections exhibit a range, of fairly considerable amount, in the magnitude of the H_{AST} and H_{MET} to 99.99 percentile H_{SUM} events, owing to the variation between projections, of extreme H. While in the future, some events still feature high fraction H_{MET} contributions the fractions become increasingly reduced as time proceeds and sea level rises.

By 2040, at both La Jolla (lower frame, **Figure 3**) and San Francisco (lower frame, **Figure 4**), there are increasing numbers and magnitude of cases for which H_{MET} contributes *negatively* to H_{SUM} . Also, as Earth warms and sea level rise continues, there tends to be diminishing contributions of H_{AST} to 99.99 percentile H_{SUM} events—i.e., a) extreme high sea levels occur with even moderate tide heights; and b) both sites begin to exhibit 99.99 percentile H_{SUM} cases where H_{MET} is only modestly high or even negative.

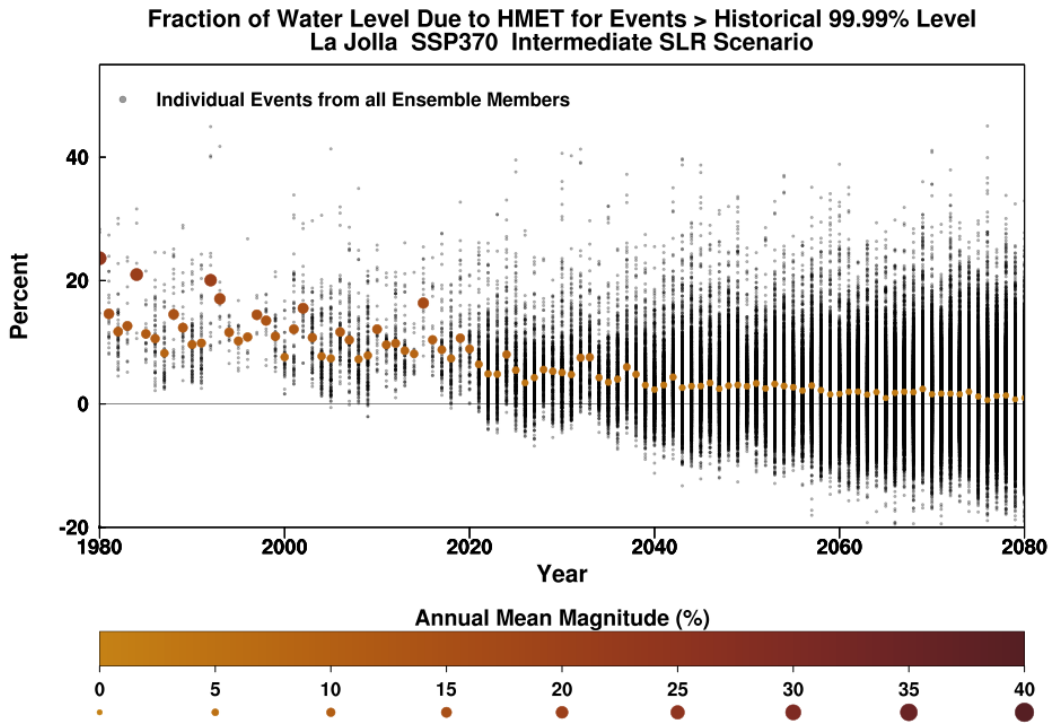
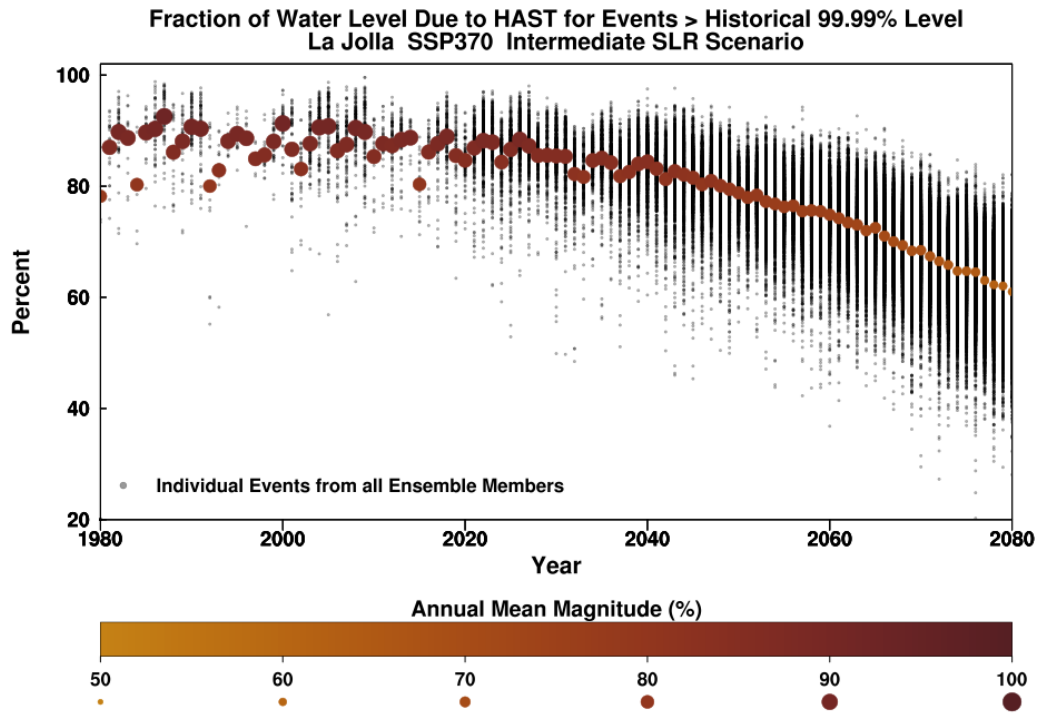


Figure 3. Contributions (fraction of total in percent) of H_{AST} and H_{MET} to 99.99 percentile H_{SUM} events, 1980 through 2080 under intermediate sea level rise scenario for La Jolla. Black dots show fractional contributions for each of the 38 CMIP6 SSP 370 projections (individual ensemble members) and brown dots show their overall mean.

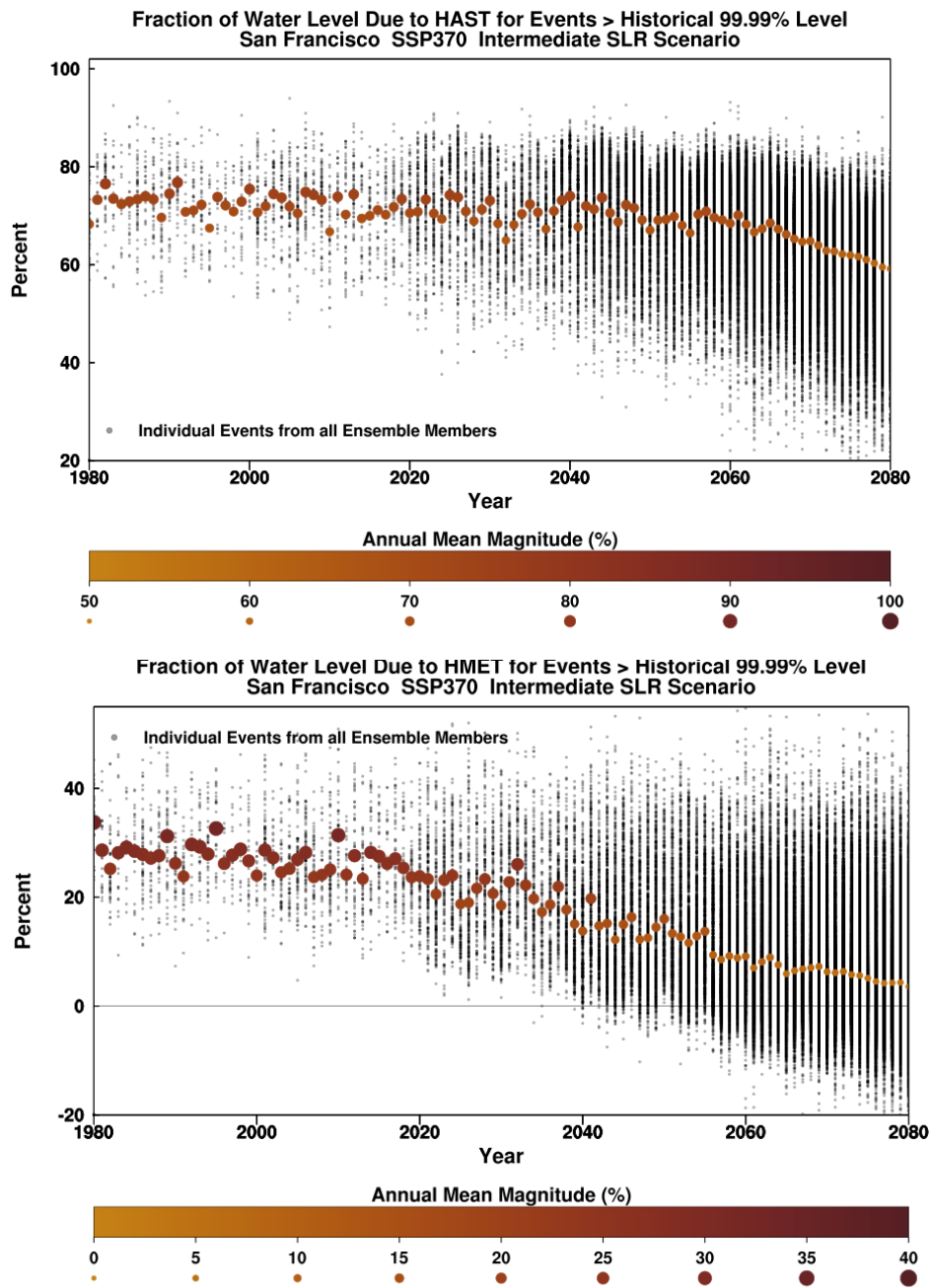


Figure 4. Contributions (fraction of total in percent) of H_{AST} and H_{MET} to 99.99 percentile H_{SUM} events, 1980 through 2080 under intermediate sea level rise scenario for La Jolla and San Francisco. Black dots show fractional contributions for each of the 38 CMIP6 SSP 370 projections (individual ensemble members) and brown dots show their overall mean.

Another view of extreme sea level events is the number of days having H_{SUM} exceeding the 99.99% threshold, shown in **Figure 5**. Under the intermediate sea level rise scenario, the number of days exhibiting extreme high sea level events increase markedly at both La Jolla and San Francisco, along with an increasing range of the number of extreme H_{SUM} days per year. From the historical period, when the 99.99 percentile H_{SUM} occurrences are limited to a bit less than

once per year, these high sea level events appear, on average, about 5 days per year by 2040 and more than 100 days per year by 2080.

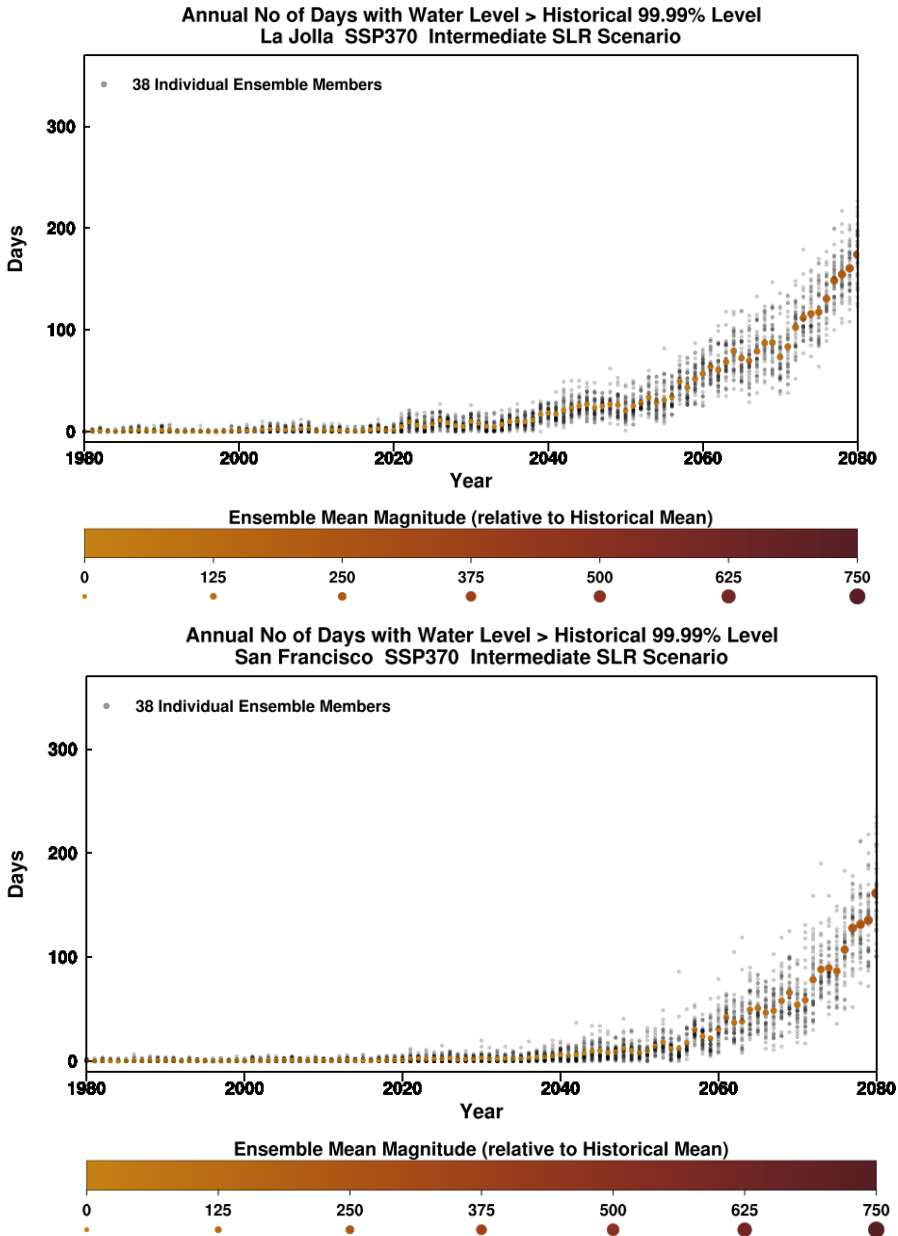


Figure 5. Number of days in each year, 1980-2080, having total sea level exceeding the historical 99.99 percentile threshold for La Jolla (above) and San Francisco (below). Black dots show number of days for each of the 38 CMIP6 SSP 370 projections for the intermediate SLR scenario and brown dots show their overall mean number of days for each year.

To evaluate how the number of events that exceed a relatively high sea level threshold would change under different sea level rise scenarios, the decade-by decade (average over 5 years) number of days having at least one hour that exceeds the historical 99.99 percentile is shown for the low, intermediate and high sea level scenarios in **Figure 6**, drawing upon the 38 individual projections using SSP 370 (ensemble members from all of the available models). Looking

carefully, by the 2020's the number of events that occur under the respective scenarios begins to separate, and by 2050 the stronger rate of increase of 99.99 percentile events within the high sea level rise scenario results in a fourfold increase over the occurrences in the low sea level rise scenario and more than a twice the number produced by the intermediate sea level rise scenario. This 5-year census also underscores the volatility of the processes that drive extreme sea level events—showing that in each 5-year period there are model projections that produce an exceptional number of days with extremely high sea levels, shown by the X's in these plots.

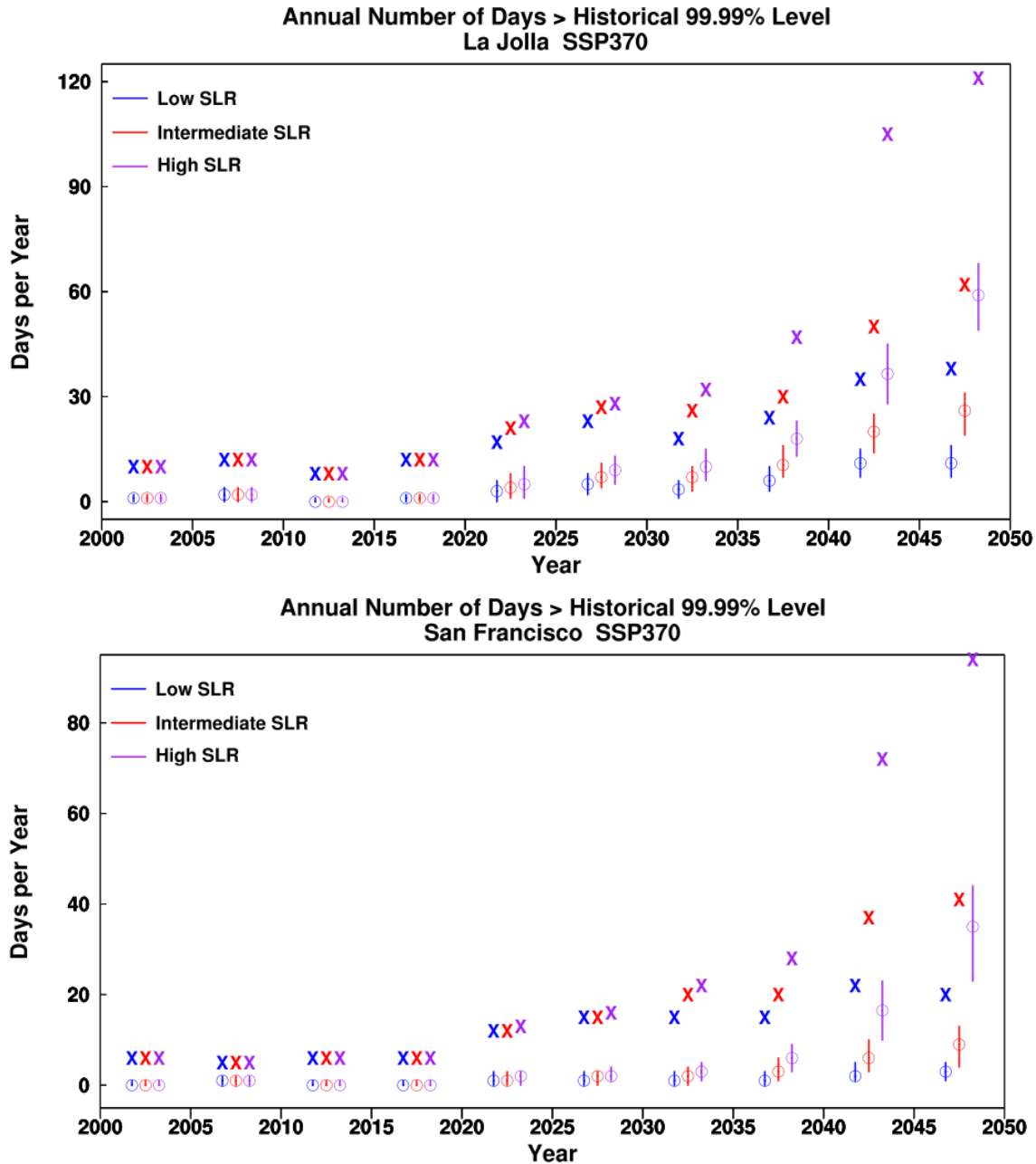


Figure 6. Five-year average number of days per year having at least one hour that exceeds the 99.99 percentile H_{SUM} for the low, intermediate, and high sea level rise (SLR) scenarios for La Jolla (upper) and San Francisco (lower). The vertical lines show the middle 50% of the distribution of the number of days obtained from each of the 38 SSP 370 individual projections (ensemble

members from all of the available models). X's show the highest number from any year in a given five-year period from the set of 38 projections.

Importantly, as the sea level rises and the number of days whose sea level reaches or exceeds the 99.99 percentile level increases, the duration (hours) of sea level above the 99.99 percentile level also increases, as shown for San Francisco in **Figure 7**. Initially, in the years through about 2040, high sea levels persist for 1 to 3 hours, but by 2080 this period grows to 8 hours or more, increasing exposure of coastal property and infrastructure to high sea levels and possible wave forces by three-fold or more.

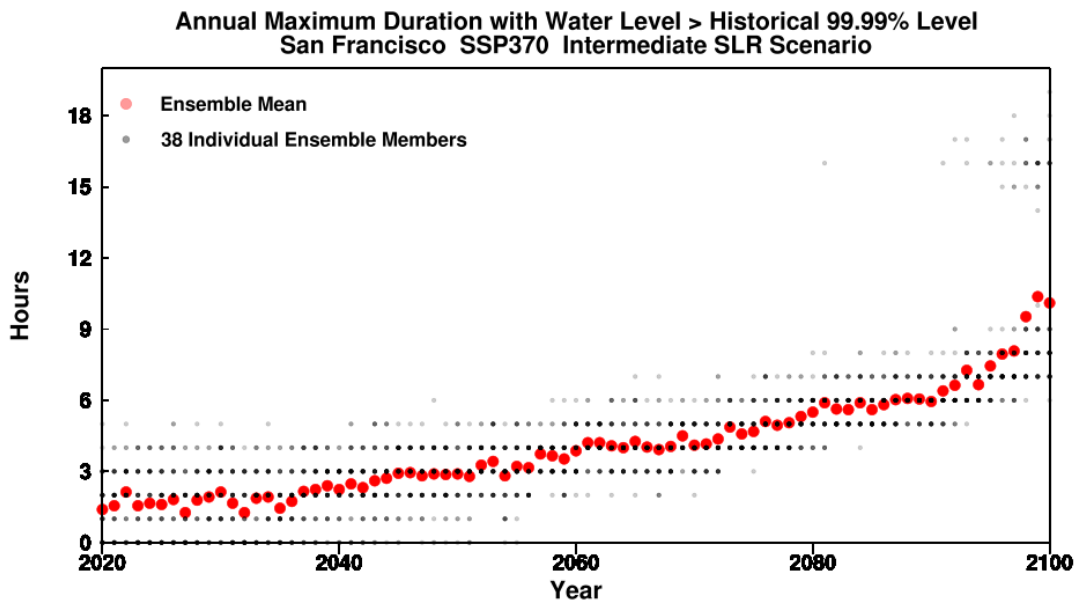


Figure 7. Duration (hours) of sea level above the 99.99 percentile level for all 99.99 percentile H_{SUM} days under the intermediate sea level rise scenario San Francisco. Black dots are obtained from the results of each of the 38 SSP 370 individual projections (ensemble members from all of the available models).

For another perspective on high sea level occurrences, the annual maximum sea level, along with the annual mean sea level for La Jolla and San Francisco is plotted for the set of SSP 370 projections under the intermediate sea level rise scenario in **Figure 8**. The trajectory of the annual maximum sea level parallels that of the annual mean sea level, rising approximately 60 cm over historical levels by 2080 at both locations, in keeping with the intermediate sea level rise scenario. At La Jolla, the annual maximum sea level ranges from about 120 to 150 cm with some exceptional cases rising to 170cm above the annual mean. At San Francisco, the annual maximum sea level ranges from about 140 to 180 cm with some exceptional cases rising to over 190cm above the annual mean. Notably, reflecting its more poleward location and the sometimes much more active weather driven H_{MET} forcing, the envelope of maximum sea level occurrences at San Francisco is considerably higher (by approximately 20cm) than that for La Jolla.

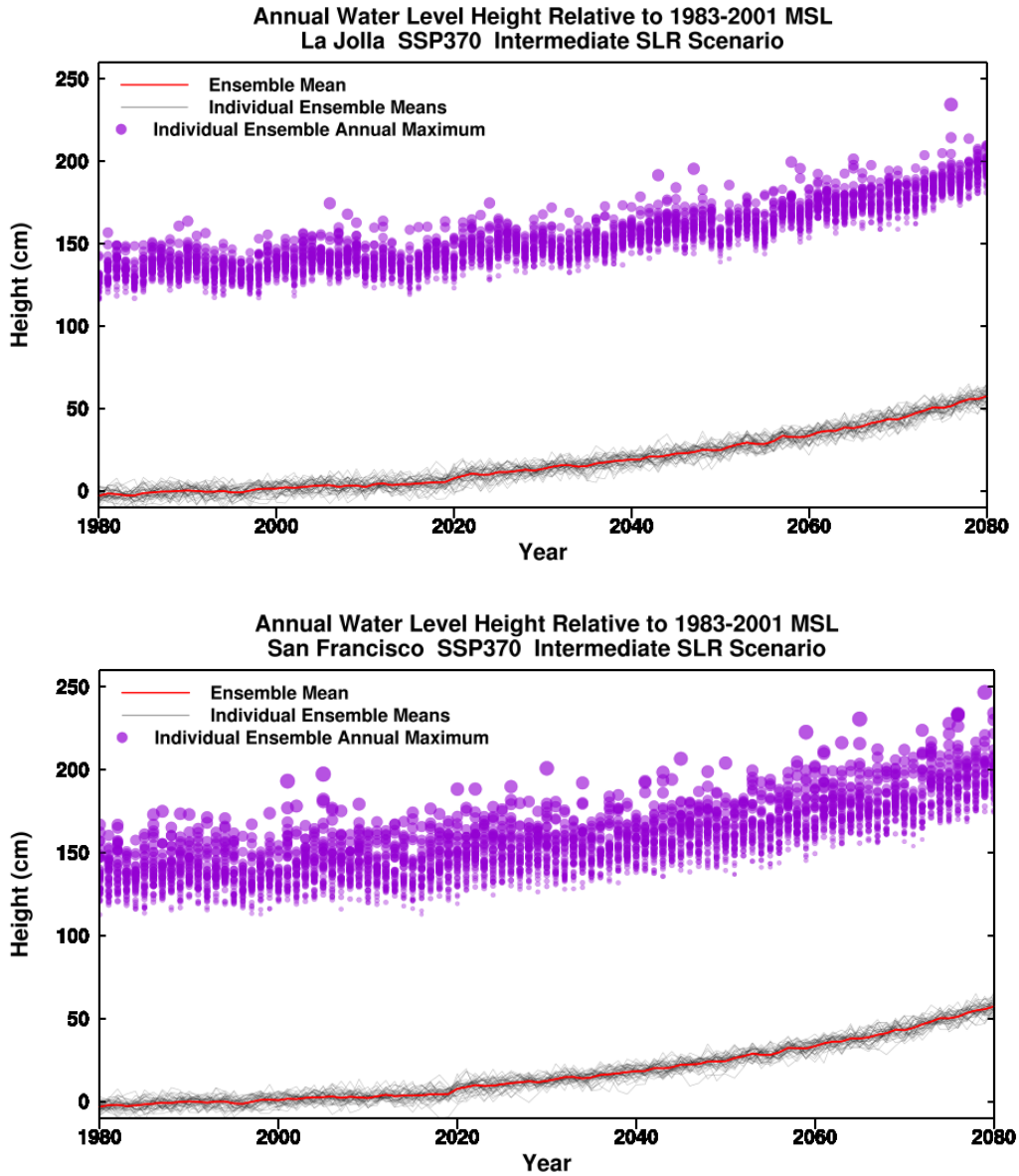


Figure 8. Projected Sea Level through 2080 for La Jolla (above) and San Francisco (below), showing the highest annual (annual extreme) value and the annual mean sea level from the 38 CMIP6 SSP 370 projections for the intermediate SLR scenario. Heights shown are relative to mean sea level (MSL) during the 1983-2001 period.

4. Guidance or Caveats on Best Practices for Use of Data Products

At the time of writing, the hourly sea level projections are available via <https://cadcat.s3.amazonaws.com/index.html#hmet/>. The associated LOCA2 downscaled CMIP6 weather and climate projections are available through the Cal-Adapt Analytics Engine (<https://analytics.cal-adapt.org>).

Each CMIP6-driven H_{MET} projection has been paired with three different (lower, medium, and higher) long-term sea-level rise scenarios. Users are advised to consider projections that might be appropriate to assess vulnerability and impacts for their particular application(s). Some of the greatest impacts of sea levels will occur during relatively short period events, so users may wish to consider occurrences in the projected sea level series when multiple factors (e.g., high tides, large storms, and El Niño conditions) converge to create high sea level extremes. Several projections of sea level, e.g. for the intermediate SLR scenario in Figure 3, are provided at each location. The ensemble of projections may allow users to assess future possibilities such as the future occurrence of high hourly sea level extremes (e.g., Figure 5). The hourly sea level projections can be combined with the downscaled climate and weather projections to investigate the time evolution of compounding weather and climate factors within the respective projections, such as co-occurring extremes of sea level and terrestrial runoff.

References

- Bromirski, P. D., Flick, R. E., & Cayan, D. R. (2003). Storminess variability along the California coast: 1858-2000. *Journal of Climate*, 16(6), 982–993. [https://doi.org/10.1175/1520-0442\(2003\)016<0982:svatcc>2.0.co;2](https://doi.org/10.1175/1520-0442(2003)016<0982:svatcc>2.0.co;2)
- Bromirski, P. D., & Flick, R. E. (2008). Storm surge in the San Francisco Bay/Delta and nearby coastal locations. *Shore & Beach*, 76(3), 29–37.
- Bromirski, P. D., Flick, R. E., & Miller, A. J. (2017). Storm surge along the Pacific coast of North America. *Journal of Geophysical Research-Oceans*, 122(1), 441–457.
- California Ocean Protection Council, California Ocean Science Trust (2024): California Sea Level Rise Guidance (2024) Science and Policy Update. 2024. California Sea Level Rise Science Task Force. <https://opc.ca.gov/wp-content/uploads/2024/05/California-Sea-Level-Rise-Guidance-2024-508.pdf>
- Cayan, D. R., P. D. Bromirski, K. Hayhoe, M. Tyree, M. D. Dettinger, and R. E. Flick (2008), Climate change projections of sea level extremes along the California coast, *Clim. Change*, 87, 57–73, doi:10.1007/s10584-007-9376-7
- Flick, R. E. (1986). A Review of Conditions Associated with High Sea Levels in Southern-California. *Science of the Total Environment*, 55, 251–259. [https://doi.org/10.1016/0048-9697\(86\)90184-1](https://doi.org/10.1016/0048-9697(86)90184-1)
- Flick, R.E. (1998), Comparison of tides, storm surges, and mean sea level during the El Niño winters of 1982–83 and 1997–98, *Shore & Beach*, 66, 7-17.

Flick, R.E. (2000), Time-of-day of peak tides in a mixed-tide regime, *Shore & Beach*, 68, 15-17.

Flick, R. E., Murray, J. F., & Ewing, L. C. (2003). Trends in United States tidal datum statistics and tide range. *Journal of Waterway Port Coastal and Ocean Engineering-Asce*, 129(4), 155–164.

Fox-Kemper, B., H.T. Hewitt, C. Xiao, G. Aðalgeirsdóttir, S.S. Drijfhout, T.L. Edwards, N.R. Golledge, M. Hemer, R.E. Kopp, G. Krinner, A. Mix, D. Notz, S. Nowicki, I.S. Nurhati, L. Ruiz, J.-B. Sallée, A.B.A. Slangen, and Y. Yu (2021): Ocean, Cryosphere and Sea Level Change. In *Climate Change 2021: The Physical Science Basis. Contribution of Working Group I to the Sixth Assessment Report of the Intergovernmental Panel on Climate Change* [Masson-Delmotte, V., P. Zhai, A. Pirani, S.L. Connors, C. Péan, S. Berger, N. Caud, Y. Chen, L. Goldfarb, M.I. Gomis, M. Huang, K. Leitzell, E. Lonnoy, J.B.R. Matthews, T.K. Maycock, T. Waterfield, O. Yelekçi, R. Yu, and B. Zhou (eds.)]. Cambridge University Press, Cambridge, United Kingdom and New York, NY, USA, pp. 1211–1362, doi: [10.1017/9781009157896.011](https://doi.org/10.1017/9781009157896.011).

Hersbach, H., Bell, B., Berrisford, P., Biavati, G., Horányi, A., Muñoz Sabater, J., Nicolas, J., Peubey, Cl., Radu, R., Rozum, I., Schepers, D., Simmons, A., Soci, C., Dee, D., Thépaut, J.-N., (2023): ERA5 hourly data on single levels from 1940 to present. Copernicus Climate Change Service (C3S) Climate Data Store (CDS), DOI: 10.24381/cds.adbb2d47.

IPCC (2021): *Climate Change 2021: The Physical Science Basis. Contribution of Working Group I to the Sixth Assessment Report of the Intergovernmental Panel on Climate Change*[Masson-Delmotte, V., P. Zhai, A. Pirani, S.L. Connors, C. Péan, S. Berger, N. Caud, Y. Chen, L. Goldfarb, M.I. Gomis, M. Huang, K. Leitzell, E. Lonnoy, J.B.R. Matthews, T.K. Maycock, T. Waterfield, O. Yelekçi, R. Yu, and B. Zhou (eds.)]. Cambridge University Press, Cambridge, United Kingdom and New York, NY, USA, In press, doi:[10.1017/9781009157896](https://doi.org/10.1017/9781009157896).

Pierce, D. W., J. F. Kalansky, and D. R. Cayan, (2018). *Climate, Drought, and Sea Level Rise Scenarios for the Fourth California Climate Assessment*. California’s Fourth Climate Change Assessment, California Energy Commission. Publication Number: CNRA-CEC-2018-006.

Pierce et al. (2023), California Hybrid Downscaling Data Justification Memo, prepared for adoption by California’s Fifth Climate Change Assessment.
https://www.energy.ca.gov/sites/default/files/2024-03/04_HybridDownscaling_DataJustificationMemo_Pierce_Adopted_ada.pdf

Sweet, W.V., B.D. Hamlington, R.E. Kopp, C.P. Weaver, P.L. Barnard, D. Bekaert, W. Brooks, M. Craghan, G. Dusek, T. Frederikse, G. Garner, A.S. Genz, J.P. Krasting, E. Larour, D. Marcy, J.J. Marra, J. Obeysekera, M. Osler, M. Pendleton, D. Roman, L. Schmied, W. Veatch, K.D. White, and C. Zuzak (2022): *Global and Regional Sea Level Rise Scenarios for the United States: Updated Mean Projections and Extreme Water Level Probabilities Along U.S. Coastlines*. NOAA Technical Report NOS 01. National Oceanic and Atmospheric Administration, National Ocean Service, Silver Spring, MD, 111 pp.

<https://oceanservice.noaa.gov/hazards/sealevelrise/noaa-nostechrpt01-global-regional-SLR-scenarios-US.pdf>

Thompson, P.R., Widlansky, M.J., Hamlington, B.D., et al. (2021) Rapid increases and extreme months in projections of United States high-tide flooding. *Nat. Clim. Chang.* **11**, 584–590.
<https://doi.org/10.1038/s41558-021-01077-8>

Zetler, B. D., and R. E. Flick (1985), Predicted extreme high tides for mixed-tide regimes, *J. Phys. Oceanogr.*, 15(3), 357–359. *Journal of Geophysical Research: Oceans*
10.1002/2016JC012178